Available online at www.sciencedirect.com
ScienceDirect
Physica C 467 (2007) 80–84
PHYSICA C
www.elsevier.com/locate/physc

Current–voltage characteristics of break junctions of high-T_c superconductors

D.M. Gokhfeld *, D.A. Balaev, K.A. Shaykhutdinov, S.I. Popkov, M.I. Petrov

L.V. Kirensky Institute of Physics SD RAS, Krasnoyarsk 660036, Russia

Received 10 April 2007; accepted 5 September 2007
Available online 14 September 2007

Abstract

The current–voltage (*I–V*) characteristics of break junctions of polycrystalline $La_{1.85}Sr_{0.15}CuO_4$, $Y_{0.75}Lu_{0.25}Ba_2Cu_3O_{7-\delta}$, $Bi_{1.8}Pb_{0.3}Sr_{1.9}Ca_2Cu_3O_x$ and composite $YBa_2Cu_3O_{7-\delta} + Ag$ are investigated. The experimental *I–V* curves exhibit the specific peculiarities of superconductor/normal-metal/superconductor junctions. The relation between an *I–V* characteristic of network of weak links and *I–V* dependencies of typical weak links is suggested to describe the experimental data. The *I–V* curves of typical weak links are calculated by the Kümmel–Gunsenheimer–Nicolsky model considering the multiple Andreev reflections.

PACS: 74.25.Fy; 74.45.+c; 74.81.Fa

Keywords: Network of weak links; Andreev reflection; Hysteretic peculiarity

1. Introduction

Measurements of current–voltage (*I–V*) characteristics are accompanied with the heat emission and the selfheating. The selfheating can modify dramatically the resulting *I–V* curve. A heat hysteresis of *I–V* curve and a dependence of *I–V* curve on the scanning velocity of current are signs of selfheating.

A removal of the selfheating is very important for transport measurements of high-T_c superconductors because their heightened temperature sensibility. By reducing the cross section S of a bulk sample one can measure *I–V* curve at a certain range of the current density for the smaller values of the measuring current. The selfheating decreases as well. In the case of non-tunneling break junction (BJ) technique, a significant reducing of S is achieved by the formation of a microcrack in a bulk sample. The non-tunneling BJ of high-T_c superconductors represents two massive polycrystalline banks connected by a narrow bottleneck (Fig. 1a). The bottleneck is constituted by granules and intergranular boundaries which are weak links (Fig. 1b). The current density in the bottleneck is much larger than that in the banks. If the bias current I is less than the critical current I_c of the bulk sample then the weak links in the banks have zero resistance. Provided small transport currents, (i) I_c and the *I–V* curve of the BJ are determined by the weak links in the bottleneck only, (ii) the selfheating effect is negligible.

The experimental *I–V* curves of BJs of high-T_c superconductors have rich peculiarities reflecting physical mechanisms of a charge transport through weak links. It was a topic of many investigations [1–6]. Here we analyze the earlier works of our group [4–6] and the new experimental data (Section 2). The model for description of the *I–V* curves is suggested in Section 3. The peculiarities observed on the experimental *I–V* curves of BJs have been explained in Section 4. Also the parameters of weak links in the investigated samples are estimated in Section 4.

2. Experimental

$La_{1.85}Sr_{0.15}CuO_4$ (LSCO), $Y_{0.75}Lu_{0.25}Ba_2Cu_3O_{7-\delta}$ (YBCO) and $Bi_{1.8}Pb_{0.3}Sr_{1.9}Ca_2Cu_3O_x$ (BSCCO) were

* Corresponding author. Tel.: +7 3912 494838.
E-mail address: gokhfeld@iph.krasn.ru (D.M. Gokhfeld).

0921-4534/$ - see front matter © 2007 Elsevier B.V. All rights reserved.
doi:10.1016/j.physc.2007.09.001

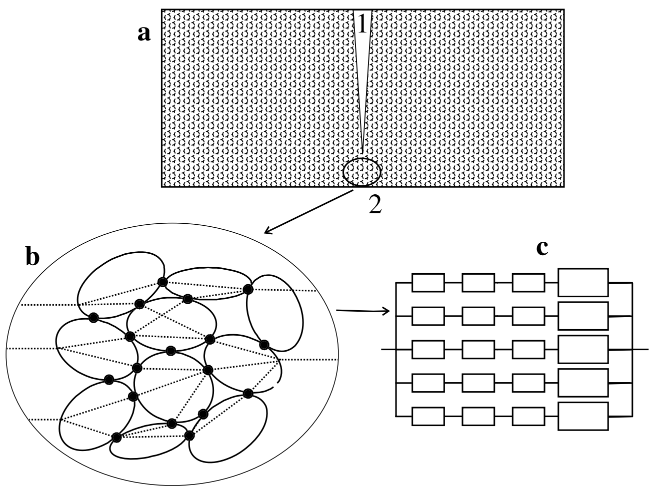

Fig. 1. (a) Break junction of polycrystalline sample. The crack 1 and the bottleneck 2 are displayed, (b) Granules in the bottleneck. Filled circles mark weak links that are intergranular boundaries. Dotted lines are the main paths for transport current, and (c) simplified circuit for the network (Section. 3.1).

synthesized by the standard ceramic technology. The composite 67 vol.% $YBa_2Cu_3O_{7-\delta}$ + 33 vol.% Ag (YBCO + Ag) was prepared from $YBa_2Cu_3O_{7-\delta}$ powder and ultradispersed Ag [7]. The initial components were mixed and pressed. Then the composite was synthesized at 925 °C for 8 h. The critical temperatures T_c are 38 K for LSCO, 112 K for BSCCO, 93.5 K for YBCO and YBCO + Ag.

Samples with a typical size of 2 mm × 2 mm × 10 mm were sawed out from synthesized pellets. Then the samples were glued to a sapphire substrates. The sapphire was chosen due to its high thermal conductivity at low temperatures. The central part of the samples was polished down to obtain a cross-sectional area $S \approx 0.2 \times 1\ \mathrm{mm}^2$. For such a value of S, the critical current I_c of YBCO and BSCCO has a typical value about 2 A at 4.2 K (current density ≈ 1000 A/cm^2). Further controllable decrease in S is very difficult due to an inevitable mechanical stresses breaking the sample. In order to obtain a contact of the break junction type, the sample with the above value of S was bent together with the substrate with the help of screws of spring-loaded current contacts. It led to the emergence of a microcrack in the part of sample between the potential contacts. As a result, either a tunneling contact (no bottleneck, the resistance $R > 10\ \Omega$ at the room temperature) or a metal contact ($R < 10\ \Omega$) was formed. Only the metal contacts were selected for investigation.

The drop of I_c (4.2 K) and the increase of R above T_c when the sample was cracked shows that the values of S decreased by ≈30 times for LSCO and ≈100 times for YBCO and BSCCO. For YBCO + Ag I_c(77.4 K) decreases by ~500 times.

The I–V curves were measured by the standard four probe technique under bias current. A typical $V(I)$ dependence of BJ has the hysteretic peculiarity which decreases as temperature increases. Also there is the excess current on the I–V curves. The I–V curves of LSCO and BSCCO BJs exhibit an arch-like structure at low temperature. The I–V curves of BJs investigated are independent of the scanning velocity of bias current. Thus, the experimental conditions provides that the hysteretic peculiarity on these I–V curves is not caused by the selfheating.

3. Model

3.1. I–V curve of network

A polycrystalline high-T_c superconductor is considered to be the network of weak links. The I–V curve of a network is determined by the I–V curves of individual weak links and their mutual disposition.

Let us consider firstly an influence of mutual disposition of weak links on the I–V curve. For a bulk high-T_c superconductor the I–V curve resembles the one of typical single weak link [8]. However the I–V curves of BJs are distorted usually in comparison with the one of a single weak link. It is because the combination of finite number of weak links remains in the bottleneck of BJ (Fig. 1a, b). So the contribution of different weak links to the resulting I–V curve is more stronger in a BJ than in a large network. The characteristics of a chaotic network is difficult to calculate [8]. To simplify the calculation of resulting I–V curve of BJ we consider an equivalent network: the simple parallel connection of a few chains of series-connected weak links (Fig. 1c). Indeed there are percolation clusters [9] in a network that are paths for current (Fig. 1b). The each percolating cluster in the considered network is considered to be the series-connected weak links.

The $V(I)$ dependence of the series-connected weak links is determined as $V(I) = \sum V_i(I)$, where the sum is over all weak links in the chain, $V_i(I)$ is the I–V curve of each weak link. The weak links and their I–V curves may be different. It is conveniently to replace here the sum over all weak links with the sum of a few more typical weak links multiplied by a weighting coefficient P_i. The relation for the series-connected weak links is resulted:

$$V(I) = N_V \sum_i P_i V_i(I), \qquad (1)$$

where N_V is the number of typical weak links, P_i shows the share of ith weak link in the resulting I–V curve of the chain, $\sum P_i = 1$.

The parallel connection of chains is considered further. If the current I flows through the network then the current I_j through jth chain equals $IP_{\|j}/N_\|$ and $\sum I_j = I$. Here $N_\|$ is the number of parallel chains in the network, $P_{\|j}$ is the weighting coefficient determined by the resistance of jth chain, $\sum P_{\|j} = 1$.

An addition (a subtraction) of chains in parallel connection smears (draws down) the I–V curve of network to higher (lower) currents. It is like to the modification of I–V curve due to the increase (the decrease) of cross section of sample. For the sake of simplicity the difference of parallel chains can be neglected and the typical chain may be considered only. Then the expression for *I–V* curve of network of weak links follows:

$$V(I) = N_V \sum_i P_i V_i \left(\frac{I}{N_{\parallel}}\right), \tag{2}$$

where the sum is over the typical weak links with weighting coefficients P_i, N_V is the number of series-connected weak links in the typical chain in the network, $I/N_{\parallel} = I_i$ is the current through the *i*th weak link of the typical chain.

3.2. I–V curve of a typical weak link

The metal intergranular boundaries were revealed in the polycrystalline YBCO synthesized by the standard ceramic technology [10]. The excess current and other peculiarities on the *I–V* curves of the studied samples are characteristic for superconductor/normal-metal/superconductor (SNS) junctions [11]. These facts verify that the intergranular boundaries in the high-T_c superconductors investigated are metallic. Therefore the networks of SNS junctions are realized in the samples under investigation.

The Kümmel–Gunsenheimer–Nicolsky (KGN) theory [12] only among theories developed for SNS structures predicts the hysteretic peculiarity on the *I–V* curve of weak link. The KGN theory considers the multiple Andreev reflections of quasiparticles. According to the KGN model, the hysteretic peculiarity reflects a part of *I–V* curve with a negative differential resistance which can be observed under bias voltage [11,12]. The KGN approach was used earlier to the description of experimental *I–V* curves of low-T_c [13,14] and high-T_c weak links [15,13].

The approach based on consideration of the phase slip in nanowires [16] may alternatively be employed to compute the hysteretic *I–V* curve. The model [16] is valid at $T \approx T_c$ while the KGN model is appropriate at temperature range $T < T_c$.

We use the simplified version of the KGN theory [12] developed in work [13] to describe the *I–V* curves of individual weak links. According to the model [13] the expression for the current density of SNS junction is given by:

$$j(V) = \sum_n \exp\left(-\frac{d}{l}n\right) \times \left\{ \frac{em^{*2}d^2}{2\pi^3\hbar^5} \int_{-\Delta+neV}^{\Delta} \mathrm{d}E \frac{|E|\sqrt{\Delta^2 - E^2}}{\left(1 - C^{\frac{2|E|}{\pi\Delta}}\right)^3} \tanh\left(\frac{E}{2k_B T}\right) + \frac{ek_F^2}{4\pi^2\hbar} \int_{E_1}^{\Delta+eV} \mathrm{d}E \frac{E}{\sqrt{E^2 - \Delta^2}} \tanh\left(\frac{E}{2k_B T}\right) \right\} + \frac{V}{R_N A} \tag{3}$$

with $C = \pi/2(1 - d\,m^*\Delta/2\hbar^2 k_F)$ for $C > 1$ and $C = 1$ otherwise, $E_1 = -\Delta + neV$ for $-\Delta + neV \geqslant \Delta$ and $E_1 = \Delta$ otherwise. Here A is the cross section area and d is the thickness of normal layer with the inelastic mean free path l and resistance R_N, e is the charge and m^* is the effective mass of electron, Δ is the energy gap of superconductor, n is the number of Andreev reflections which a quasiparticle with energy E undergoes before it moves out of the normal layer.

One should calculate a few *I*(*V*) dependencies by Eq. (3) for different parameters to simulate the *I–V* curve of network by Eq. (2). Almost all parameters in Eq. (3) can be dispersing for different weak links. Indeed there are some distribution functions of the parameters of intergranular boundaries (d, A, R_N) or the parameters of superconducting crystallites (Δ, the angle of orientation) in the SNS network.

4. Current–voltage characteristics

Figs. 2–5 show the experimental *I–V* curves of BJs (circles) and the calculated *I–V* curves of SNS networks (solid lines). The right scale of *V*-axis of all graphs is given in the units eV/Δ to correlate the position of peculiarities on *I–V* curve with the value of energy gap.

The parameters of superconductors are presented in Table 1. The mean values of energy gap Δ_0 at $T = 0$ known to be for high-T_c superconductors were used. Parameters k_F,m^* were estimated by the Kresin-Wolf model [17].

For a fitting we have calculated the *I*(*V*) dependencies of different SNS junctions by Eq. (3) to describe different parts of the experimental *I–V* curve. The parameters varied were d and R_N. Then we have substituted the arrays of *I–V* values to Eq. (2). The most experimental *I–V* curves are satisfactory described when the sum in Eq. (2) contains at least two members. The first member describes the hysteretic peculiarity, the second one describes the initial part of *I–V* curve. The fitting is illustrated in detail on Fig. 2 were curve 1 is calculated for $d = 78$ Å, curve 2 is calculated for $d = 400$ Å.

The main fitting parameters are d/l, N_V, $N_{\parallel A}$, $R_N/N_{\parallel}$, $P_{1,2}$. The parameter P_1 is the weighting coefficient for the

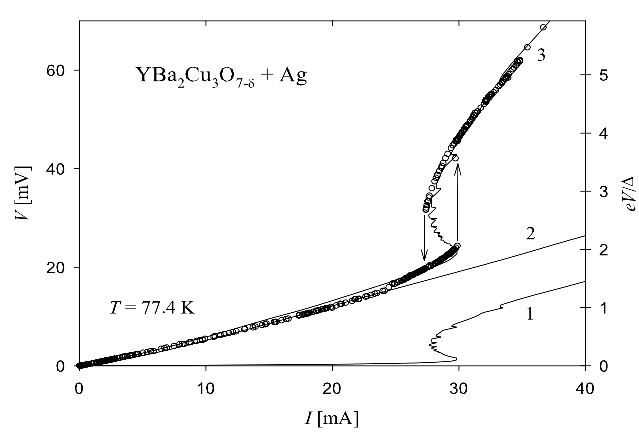

Fig. 2. *I–V* curve of YBCO + Ag break junction at $T = 77.4$ K. Experiment (circles) and computed curves (solid lines). Arrows display the jumps of voltage drop. Curve 1 that is $N_{\parallel}$ $I_1(V_1)$ fits the hysteretic peculiarity. Curve 2 that is $N_{\parallel}$ $I_2(V_2)$ fits the initial part of *I–V* curve. Curve 3 is the dependence $V(I) = N_V(P_1V_1(I/N_{\parallel}) + P_2V_2(I/N_{\parallel}))$.

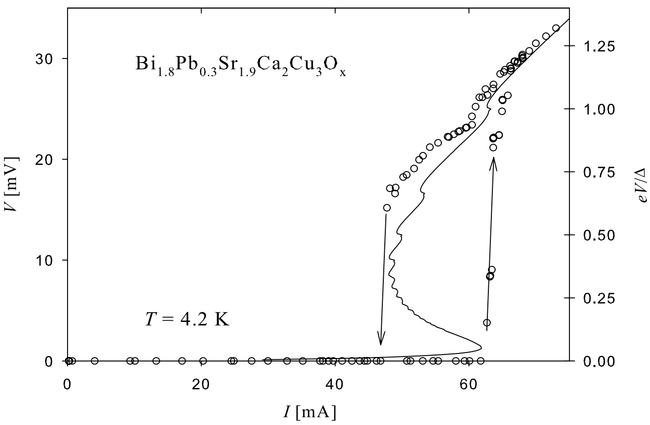

Fig. 3. I–V curve of BSCCO break junction at $T = 4.2$ K. Experiment (circles) and computed curve (solid line). Arrows display the jumps of voltage drop.

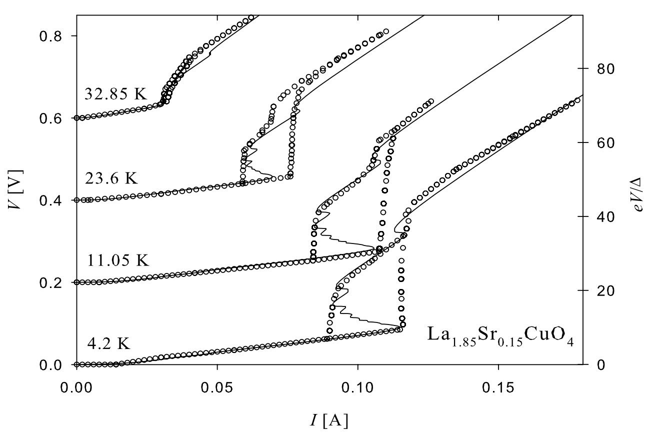

Fig. 4. Temperature evolution of I–V curve of LSCO break junction. Experiment (circles) and computed curves (solid lines). The I–V curves at 11.05 K, 23.6 K, 32.85 K are shifted up by 0.2 V, 0.4 V, 0.6 V correspondingly.

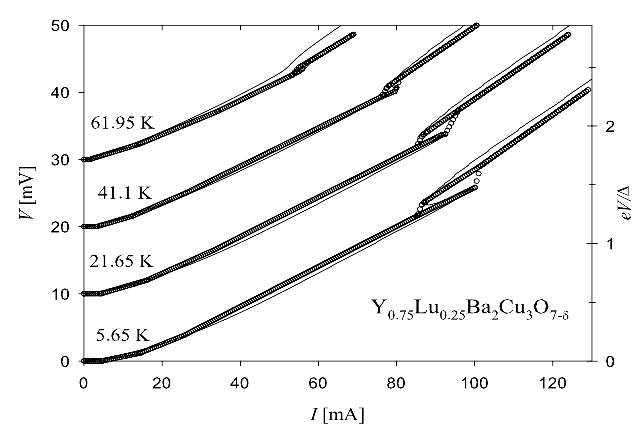

Fig. 5. Temperature evolution of I–V curve of YBCO break junction. Experiment (circles) and computed curves (solid lines). The I–V curves at 21.65 K, 41.1 K, 61.95 K are shifted up by 10 mV, 20 mV, 30 mV correspondingly.

stronger (with the thinner d) typical weak link, $P_2 = 1 - P_1$. Some parameters used are presented in Table

Table 1
Parameters of superconductors

Sample	Δ_0 [meV]	m^*/m_e	k_F [Å^{-1}]
BSCCO	25	6.5	0.61
LSCO	9	5	0.35
YBCO	17.5	5	0.65
YBCO + Ag	17.5	5	0.65

Table 2
Parameters of SNS junctions in the networks

Sample	l [Å]	d_1 [Å]	d_2 [Å]	P_1	N_V	$N_\parallel$
BSCCO	72[a]	3.5	–	1	1	1
LSCO	50[a]	4.8	20	0.905	15	20
YBCO	90[a]	2	20	0.333	3	1
YBCO + Ag	1000[b]	78	400	0.75	4	5
	100[b]	7.8	40	0.75	4	5

[a] Value at $T = 4.2$ K.
[b] Value at $T = 77.4$ K.

2. Values of l are estimated from the experimental data of resistivity (2, 3, 1.6, 3.6 mOhm cm at 150 K for bulk BSCCO, LSCO, YBCO, YBCO + Ag correspondingly) and data of works [18,19]. The value of l for Ag at 77 K is known to be ~0.1 cm. But it is more realistic to use much smaller value for composite. Table 2 shows the possible different values of l and the corresponding values of d for YBCO + Ag.

The number of the parallel paths $N_\parallel$ is estimated by assuming $A \simeq 10^{-11}$ cm^2 for the weak links in polycrystalline high-T_c superconductors. Such choice of A is reasonable because the cross section area of weak link should be more smaller than D^2 (Fig. 1b), where $D \sim 10^{-4}$ cm is the grain size of high-T_c superconductors. This rough estimation of $N_\parallel$ is influenced by a form of the percolation clusters in the sample [9] and imperfections of weak links.

Figs. 2–5 demonstrate that the hysteretic peculiarity on the experimental I–V curves is resulted from the region of negative differential resistance. This region is due to the number of the Andreev reflections decreases when the voltage increases.

The experimental I–V curves for LSCO and YBCO at different temperatures and the corresponding curves computed are presented in Figs. 4 and 5. We account a decreasing of l and Δ to compute I–V curves at higher tem- peratures (for LSCO l (11.05 K) = 50 Å, Δ (11.05 K) = 0.93 meV, l (23.6 K) = 50 Å, Δ (23.6 K) = 0.69 meV, l (32.85 K) = 47 Å, Δ (32.85 K) = 0.46 meV; for YBCO l (21.65 K) = 81 Å, Δ (21.65 K) = 17.3 meV, l (41.1 K) = 70 Å, Δ (41.1 K) = 16.6 meV, l (61.95 K) = 60 Å, Δ (61.95 K) = 13.3 meV). The coincidence of computed curves and experimental I–V curves becomes less satisfactory then T approaches to T_c. As possible, this discrepancy is due to an influence of other thermoactivated mechanisms.

As the simulation curves demonstrate (Figs. 3 and 4), the arch-like peculiarity on the experimental I–V curves of LSCO and BSCCO is one of the arches of the subharmonic gap structure [12]. By using Eq. (2) we account for the arch-like peculiarity at voltages $\gg \Delta/e$ for LSCO (Fig. 4) that should seem to contradict the KGN model prediction for the subharmonic gap structure at $V \leqslant 2\Delta/e$ [12].

Also we have used Eq. (2) to estimate the number of resistive weak links in the sample of composite 92.5 vol.% YBCO + 7.5 vol.% $BaPbO_3$ [15]. The I–V curve of this composite was described earlier by the KGN based approaches [15,13]. We obtained $N_V = 13$, $N_{\parallel} \approx 4000$ and the full number of resistive weak links is 52,000. Small number N_V is the evidence that the shot narrowest part of bulk sample is resistive only.

5. Conclusion

We have measured the I–V characteristics of break junctions of polycrystalline high-T_c superconductors. The peculiarities that are typical for SNS junctions are revealed on the I–V curves.

The expression for I–V curve of network of weak links (Eq. (2)) was suggested to describe the experimental data. Eq. (2) determines the relation between the I–V curve of network and the I–V characteristics of typical weak links.

The I–V curves of SNS junctions forming the network in the polycrystalline high-T_c superconductors are described by the Kümmel–Gunsenheimer–Nicolsky approach [12,13]. The multiple Andreev reflections are found to be responsible for the hysteretic and arch-like peculiarities on the I–V curves. The shift of subharmonic gap structure to higher voltages is explained by the connection of a few SNS junctions in series.

We believe that the expression suggested (Eq. (2)) allows to estimate the number of junctions with nonlinear I–V curves and $R > 0$ in various simulated networks.

Acknowledgements

We are thankful to R. Kümmel and Yu.S. Gokhfeld for fruitful discussions. This work is supported by program of President of Russian Federation for support of young scientists (Grant MK 7414.2006.2), program of presidium of Russian Academy of Sciences "Quantum macrophysics" 3.4, program of Siberian Division of Russian Academy of Sciences 3.4, Lavrent'ev competition of young scientist projects (project 52).

References

[1] U. Zimmermann, S. Abens, D. Dikin, K. Keck, T. Wolf, Physica B 218 (1996) 205.
[2] V.M. Svistunov, V.Yu. Tarenkov, A.I. Dyachenko, E. Hatta, JETP Lett. 71 (2000) 289.
[3] R.S. Gonnelli, A. Calzolari, D. Daghero, G.A. Ummarino, V.A. Stepanov, G. Giunchi, S. Ceresara, G. Ripamonti, Phys. Rev. Lett. 87 (2001) 097001.
[4] M.I. Petrov, D.A. Balaev, D.M. Gokhfeld, K.A. Shaikhutdinov, K.S. Aleksandrov, Phys. Solid State 44 (2002) 1229.
[5] M.I. Petrov, D.A. Balaev, D.M. Gokhfeld, K.A. Shaikhutdinov, Phys. Solid State 45 (2003) 1219.
[6] M.I. Petrov, D.M. Gokhfeld, D.A. Balaev, K.A. Shaihutdinov, R. Kümmel, Physica C 408 (2004) 620.
[7] A.G. Mamalis, S.G. Ovchinnikov, M.I. Petrov, D.A. Balaev, K.A. Shaihutdinov, D.M. Gohfeld, S.A. Kharlamova, I.N. Vottea, Physica C 364–365 (2001) 174.
[8] R. Haslinger, R. Joynt, Phys. Rev. B 61 (2000) 4206.
[9] D. Stauffer, Phys. Rep. 54 (1979) 1.
[10] M.I. Petrov, D.A. Balaev, D.M. Gokhfeld, Phys. Solid State 49 (2007) 619.
[11] K.K. Likharev, Rev. Mod. Phys. 51 (1979) 101.
[12] R. Kümmel, U. Gunsenheimer, R. Nicolsky, Phys. Rev. B 42 (1990) 3992.
[13] D.M. Gokhfeld, Supercond. Sci. Technol. 20 (2007) 62.
[14] D.M. Gokhfeld, Physica C (2007) materials of M^2S-HTSC.
[15] M.I. Petrov, D.A. Balaev, D.M. Gokhfeld, S.V. Ospishchev, K.A. Shaihutdinov, K.S. Aleksandrov, Physica C 314 (1999) 51.
[16] S. Michotte, S. Matefi-Tempfli, L. Piraux, D.Y. Vodolazov, F.M. Peeters, Phys. Rev. B 69 (2004) 094512.
[17] V.Z. Kresin, S.A. Wolf, Phys. Rev. B 41 (1990) 4278.
[18] D. Larbalestier, A. Gurevich, D.M. Feldmann, A. Polyanskii, Nature 414 (2001) 368.
[19] L.P. Gorkov, N.B. Kopnin, Usp. Fiz. Nauk 156 (1988) 117 (Sov. Phys. Usp. 31 (1988) 850).